Elsevier has created a Monkeypox Information Center in response to the declared public health emergency of international concern, with free information in English on the monkeypox virus. The Monkeypox Information Center is hosted on Elsevier Connect, the company's public news and information website.

Elsevier hereby grants permission to make all its monkeypox related research that is available on the Monkeypox Information Center - including this research content - immediately available in publicly funded repositories, with rights for unrestricted research re-use and analyses in any form or by any means with acknowledgement of the original source. These permissions are granted for free by Elsevier for as long as the Monkeypox Information Center remains active.

Virology 475 (2015) 150–158

Contents lists available at ScienceDirect

Virology

journal homepage: www.elsevier.com/locate/yviro

Comparative live bioluminescence imaging of monkeypox virus dissemination in a wild-derived inbred mouse (*Mus musculus* castaneus) and outbred African dormouse (*Graphiurus kelleni*)

Patricia L. Earl, Jeffrey L. Americo, Catherine A. Cotter, Bernard Moss*

Laboratory of Viral Diseases, National Institute of Allergy and Infectious Diseases, National Institutes of Health, Bethesda, MD 20892, United States

ARTICLE INFO

Article history:
Received 11 October 2014
Returned to author for revisions
13 November 2014
Accepted 14 November 2014
Available online 2 December 2014

Keywords:
Monkeypox virus pathogenesis
Monkeypox virus virulence
Orthopoxviruses
Animal models
Smallpox

ABSTRACT

Monkeypox virus belongs to the orthopoxvirus genus, infects rodents and monkeys in Africa, produces a smallpox-like zoonotic disease in humans, and has the potential for global spread and exploitation for bioterrorism. Several small animal models for studying monkeypox virus pathogenesis have been investigated. The African dormouse is a candidate natural host but is outbred and no immunological reagents exist. Although not a natural host, the CAST/EiJ mouse is inbred and animals and reagents are commercially available. We compared the dissemination of monkeypox virus by bioluminescence imaging in CAST/EiJ mice and dormice. In CAST/EiJ mice, intense replication occurred at the intranasal site of inoculation and virus spread rapidly to lungs and abdominal organs, which had a lower virus burden. Compared to CAST/EiJ mice, dormice exhibited a greater variation of virus spread, a slower time course, less replication in the head and chest, and more replication in abdominal organs prior to death.

Published by Elsevier Inc.

Introduction

The orthopoxviruses comprise a genus of the chordopoxvirus subfamily of the Poxviridae, which include members causing disease in humans and other animals (Damon, 2007; Essbauer et al., 2010). Variola virus, the most notorious member of this genus, is a human-specific pathogen that caused smallpox, which was eradicated more than three decades ago subsequent to global vaccination with the closely related vaccinia virus (VACV) (Fenner et al., 1988). Some orthopoxviruses, like variola virus, exhibit pronounced host specificity. Additional examples include ectromelia virus, a specific mouse pathogen (Esteban and Buller, 2005) and camelpox virus, which causes disease in camels and rarely infects humans (Bera et al., 2011). Although the original animal reservoir of VACV is unknown, zoonoses in Brazil and India are caused by strains that have become prevalent in rodents, cattle and buffalo (da Fonseca et al., 2011; Singh et al., 2012). Cowpox virus and monkeypox virus (MPXV) primarily infect rodents but can be transmitted to other animals as well as humans. Human monkeypox is most prevalent in the rain forests of central Africa, particularly the Democratic Republic of the Congo, and clinically resembles smallpox except for lower mortality and fewer human-to-human transmissions (McCollum and Damon, 2014; Parker et al., 2007). A less virulent strain of MPXV is present in West Africa and in the year 2003 was imported with infected rodents (9 African dormice, 3 rope squirrels and 2 giant pouched rats) to the United States resulting in 47 laboratory confirmed and additional clinically diagnosed human cases (Hutson et al., 2007; Reynolds and Damon, 2012). Sporadic human MPXV infections have also been detected in countries neighboring the Democratic Republic of the Congo, contributing to concerns that it may be an emerging disease. Monkeypox virus is unlikely to be eradicated because of its wide host range and the ready transmission from African to North American rodents (prairie dogs) highlights the possibility for global spread. Vaccines and therapeutics developed for control of smallpox are also effective against MPXV and the latter is being used as a surrogate for variola virus in non-human primate models (Cann et al., 2013; Johnson et al., 2011; Stittelaar et al., 2006, 2005). As the most serious communicable orthopoxvirus infection of humans, excluding variola virus, the potential exploitation of MPXV for bioterrorism has led to the designation of Congo strains as a Select Agent by the government of the United States of America (http://www.selectagents.gov).

Orthopoxviruses contain a highly conserved set of genes that are required for replication, and more variable genes that influence host range and pathogenicity (Moss, 2007). Several small animal models (Hutson and Damon, 2010; Parker and Buller, 2013), including

* Correspondence to: Laboratory of Viral Diseases, 33 North Drive, National Institutes of Health, Bethesda, MD 20892. Tel.: +1 3014969869.
E-mail address: bmoss@nih.gov (B. Moss).

http://dx.doi.org/10.1016/j.virol.2014.11.015
0042-6822/Published by Elsevier Inc.

the American black-tailed prairie dog (Guarner et al., 2004; Hutson et al., 2009; Keckler et al., 2011; Langohr et al., 2004; Xiao et al., 2005) and the thirteen-lined ground squirrel (Sbrana et al., 2007; Tesh et al., 2004), have been developed for the study of MPXV pathogenicity and to evaluate vaccines and therapeutics. Although sensitive to infection with low doses of MPXV, these wild-caught animals exhibit animal-to-animal variation and are difficult to breed in captivity. In addition, there is a dearth of immunological reagents. The African dormouse, a mouse-size rodent of the family *Gliridae,* was one of three MPXV-infected species in a shipment from West Africa (Hutson et al., 2007). African dormice can be bred in captivity, although there are no commercial sources suitable for scientific investigations and there is also a deficiency of immunological reagents (Schultz et al., 2009). Commonly used mouse strains are highly resistant to MPXV (Hutson et al., 2010) but a large screen identified several susceptible, wild-derived inbred strains (Americo et al., 2010) and one of these, the CAST/EiJ mouse, has been further studied (Earl et al., 2012). Commercial availability of animals and reagents are advantages of this model. However, there has been no detailed comparison of MPXV infection of CAST/EiJ mice with that of a natural host.

Bioluminescence imaging (BLI), an effective, non-invasive way to study virus dissemination in small animal models, has been used for VACV (Americo et al., 2014; Luker et al., 2005; Luker and Luker, 2008; Zaitseva et al., 2009). By constructing a recombinant virus expressing firefly luciferase (FL) or other luciferase enzymes, the light emitted can be used to localize sites of infection and quantify virus replication in a living animal. An important advantage of the method is that infection can be followed over days to weeks in the same animal. Osorio et al. (2009) investigated the dissemination of MPXV in BALB/c and BALB/c SCID mice following intraperitoneal inoculation. Abdominal luminescence was detected in both the normal and immunodeficient mice but systemic spread only occurred in the latter. Recently, BLI was used to follow the dissemination of MPXV in black-tailed prairie dogs following intranasal (IN) administration (Falendysz et al., 2014). Luminescence was detected in superficial regions but not in deep tissues such as lung, perhaps due to the size of the animals. The purpose of the present study was to use BLI to compare MPXV infections of the susceptible CAST/EiJ mouse, the resistant BALB/c mouse and the African dormouse. We chose to use IN infection as upper respiratory and mucosal routes seem likely for human to human spread in both smallpox (Fenner et al., 1988) and human monkeypox (Reynolds et al., 2006). However, the modes of spread of MPXV between rodents and from rodents to humans are uncertain.

Results

Construction and characterization of recombinant MPXV expressing FL

Insertion of the FL open reading frame (ORF) between the F12 and F13 ORFs of VACV strain WR has been shown to have no or minimal effects on virus replication in cell culture or virulence in mice (Americo et al., 2014; Luker et al., 2005). Similarly, we introduced the FL ORF controlled by a strong synthetic VACV early/late promoter between, and in the same orientation as, the MPXV 044 and 045 ORFs (homologous to VACV F12 and F13). Several virus clones were isolated by limiting dilution and three rounds of plaque purification. The

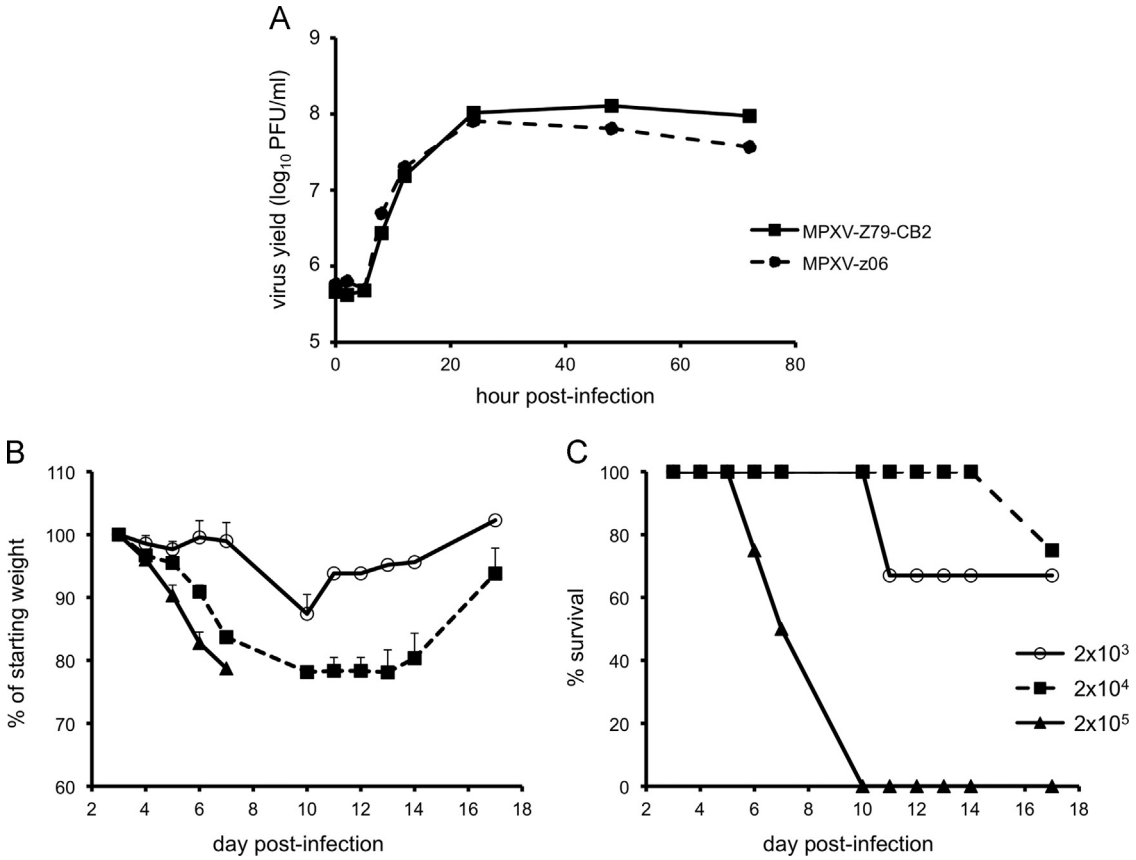

Fig. 1. In vitro and in vivo characterization of MPXV-z06. (A) Growth curves. BSC-1 cells were infected with 3 PFU per cell of the parental virus (MPXV-Z79-CB2) or the recombinant virus expressing FL (MPXV-z06). At various times after infection, cells from triplicate wells were harvested and lysed, and titers were determined by plaque assay. (B and C) Weight loss and survival of CAST mice infected with MPXV-z06. Groups of three or four 9-week old female mice were infected IN with doses of MPXV-z06 between 2×10^3 and 2×10^5 PFU. Animals were monitored for weight loss (B) and death (C) for 18 days.

recombinant clones and parental virus made plaques of similar size and appearance and one isolate, MPXV-ZFL-06 (abbreviated MPXV-z06), was chosen for further characterization. A one-step growth curve was performed on BS-C-1 cells, and virus titers were determined at successive times after infection. The kinetics of infectious virus formation was similar for MPXV-z06 and the parental virus (Fig. 1A).

Virulence of MPXV-z06 for CAST/EiJ mice

Groups of mice were infected with 2×10^3, 2×10^4 or 2×10^5 plaque forming units (PFU) of MPXV-z06 by the IN route. Mice infected with 2×10^5 PFU became lethargic, exhibiting hunched posture, ruffled fur, and severe weight loss within a few days and died between days 6 and 10 (Fig. 1B and C), mimicking the fate of CAST/EiJ mice infected with the parental virus (Americo et al., 2010). At the lower doses of 2×10^4 and 2×10^3 PFU, the animals experienced less severe disease with maximum weight losses of 22% and 13%, respectively (Fig. 1B). One mouse in both the 2×10^4 and 2×10^3 PFU groups succumbed to the MPXV infection (Fig. 1C). Although the MPXV-z06 was pathogenic, the lower doses produced less disease than that previously reported for the parental virus (Americo et al., 2010). However, the data are not directly comparable because the animals in the present study were 3 to 4 weeks older than in the previous one and resistance to MPXV increases with age (our unpublished results).

Kinetics of MPXV-z06 spread in CAST/EiJ mice

To follow virus dissemination and replication over time, CAST/EiJ mice were infected IN with 2×10^4 or 2×10^5 PFU of MPXV-z06. Beginning on day 3 post-infection, animals were imaged every weekday until death or clearance of virus. Pseudocolor images, with luminescence intensity increasing from violet to red are shown. The kinetics of virus spread in animals infected at the lower dose is shown in Fig. 2. Due to the very high amount of luminescence in the nasal area, animals were also imaged after covering the head and thus lowering the threshold for visualizing luminescence in the chest and abdomen. Accordingly, the heads and bodies are shown separately in Fig. 2. Regions of interest (ROI) as depicted in animal 901 RP on day 21 were drawn around the head, chest, and abdomen and photon flux was calculated. Replication in the nasal area was evident on day 3, increased daily, and peaked between days 7 and 12. Three of the 4 animals (901 RP, 901 LP, and 901 NP) demonstrated a diminution of photon flux in the head between days 12 and 17 and subsequently cleared the virus and recovered. In the fourth animal, luminescence reached a maximum on day 7 but did not substantially decrease and death occurred on day 14. The photon flux in the chest and abdomen also increased between days 3 and 7 and then gradually declined in the three surviving animals. Although the photon flux values were similar for the chest and abdomen, MPXV replication was

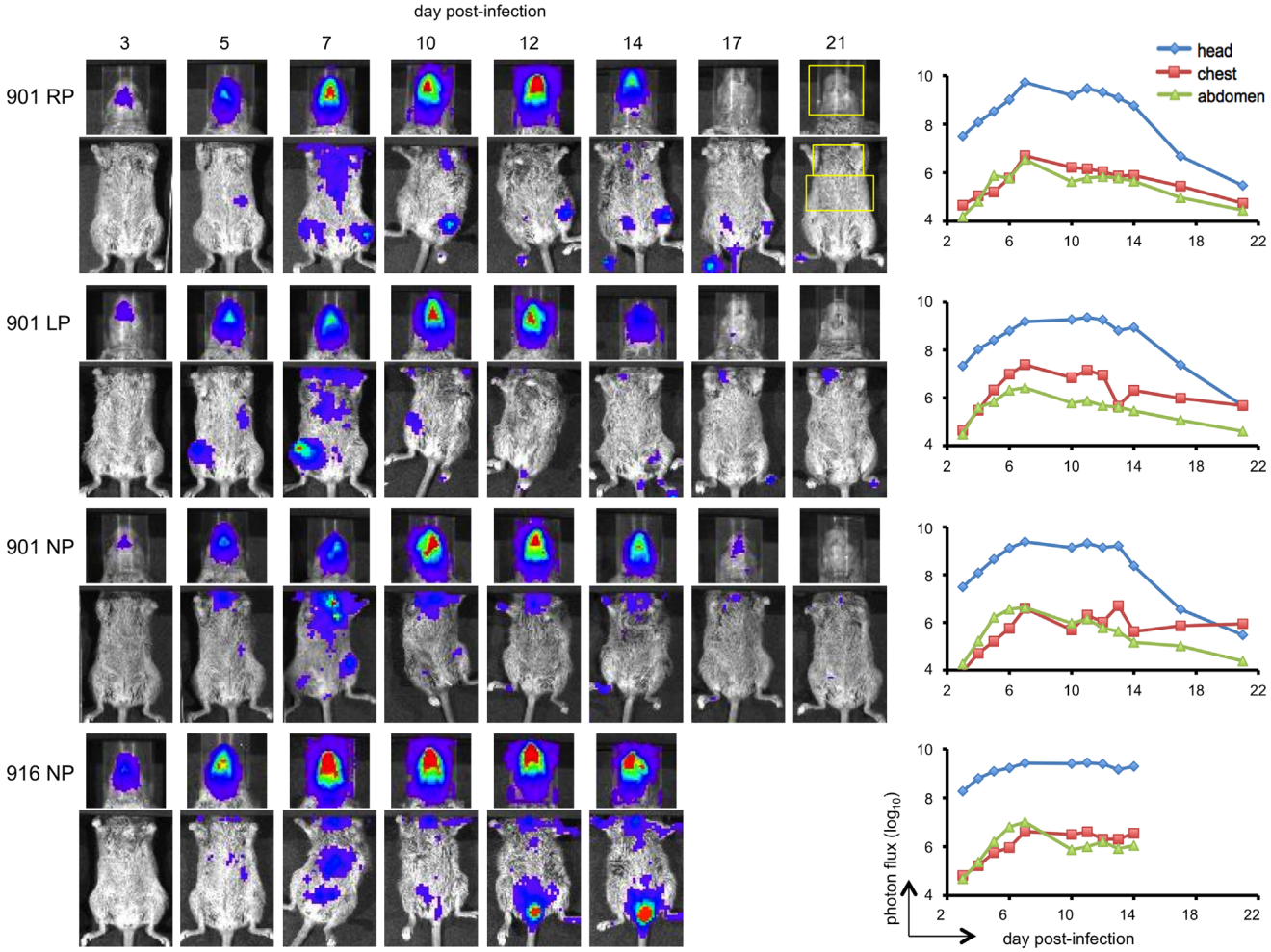

Fig. 2. Bioluminescence imaging of CAST/EiJ mice infected with 2×10^4 PFU of MPXV-z06. Four 9-week old female CAST/EiJ mice were infected IN and imaged daily on weekdays from day 3 to day 21 post-infection. Images from representative days are shown. Exposure times were 1 s, bin=8 for the head. Exposures of the body were 30 s at bin=16 with black paper covering the head. Red, blue, and purple denote intensity of luminescence from high to low. Regions of interest defining the head, chest, and abdomen (yellow boxes in animal 901 RP) were used to determine the total photon flux using Living Image software.

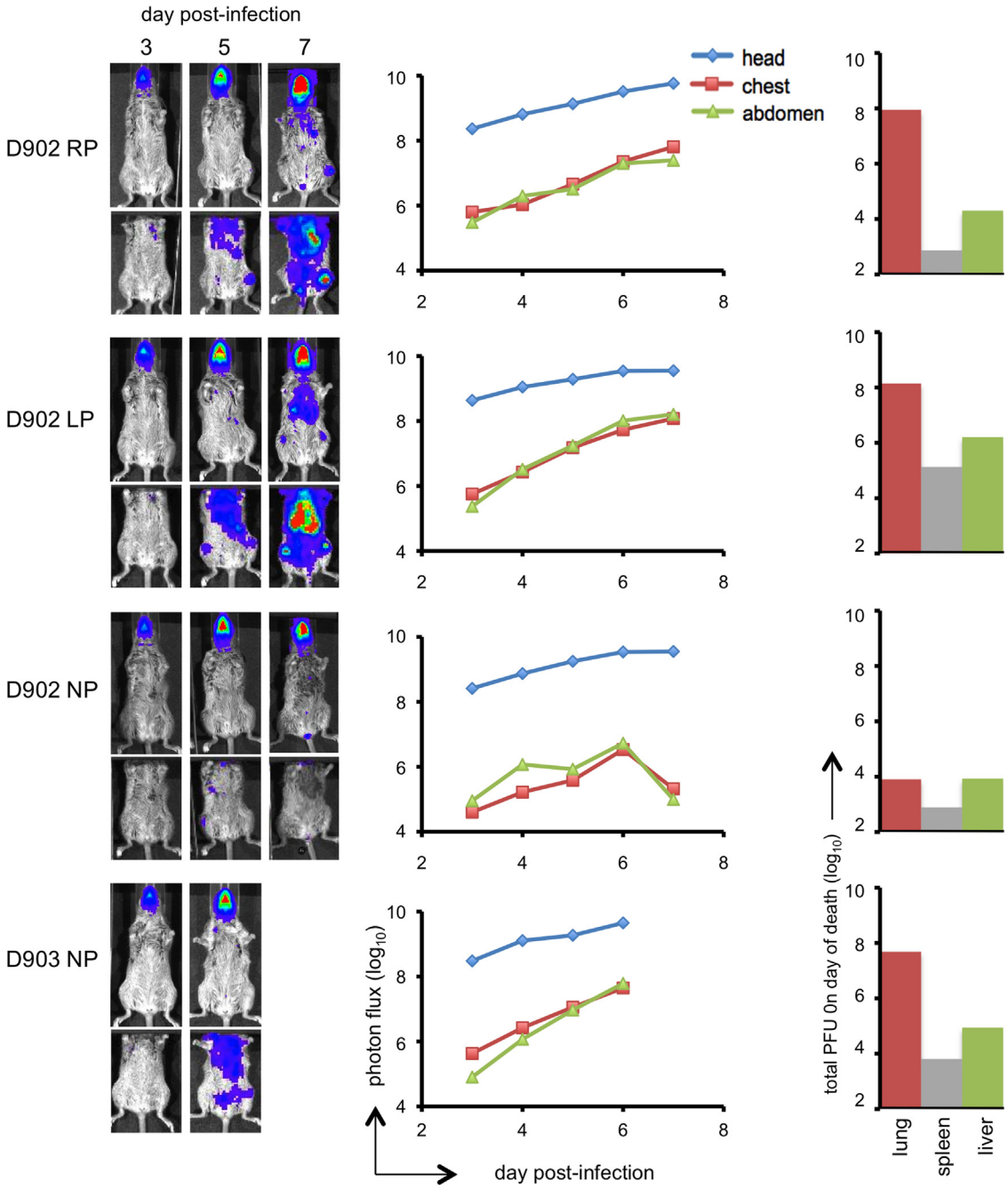

Fig. 3. Bioluminescence imaging of CAST/EiJ mice infected with 2×10^5 PFU of MPXV-z06. Four 9-week old female CAST/EiJ mice were infected IN and imaged daily on weekdays from day 3 post-infection until death. Exposures of the entire body were 1 s at bin = 8. Exposures of the body with the head covered were 30 s at bin = 16. Red, blue, and purple denote intensity of luminescence from high to low. Regions of interest defining the head, chest, and abdomen (as shown in Fig. 2) were used to determine the total photon flux. On the day of death, organs were removed and virus titers determined by plaque assay.

greater in the lung than liver and spleen due to the anatomically related difference in attenuation of photon emission (see below and unpublished data).

The CAST/EiJ mice infected with the higher dose of 2×10^5 PFU were similarly imaged (Fig. 3). Luminescence in all 3 areas of the body was higher at this dose than in animals infected at 2×10^4 PFU and did not decrease with time. All animals succumbed by day 10 post-infection and the lungs, livers, and spleens were removed for virus titration. Despite the similar photon flux in the chest and abdomen, the yields of virus from the lungs were several logs higher than from liver or spleen. There was a good correlation ($r^2 > 0.95$) between photon flux and virus yield in the chest.

Kinetics of MPXV-z06 spread in BALB/c mice

We also imaged MPXV spread in highly resistant BALB/c mice for comparison. These classical inbred mice exhibit only minor weight loss and no deaths even at a dose of 10^6 PFU. Nevertheless, we previously showed that replication in the lungs of BALB/c mice is robust, reaching levels similar to CAST/EiJ mice on days 4 to 6 post-infection (Earl et al., 2012). However, there was little spread of MPXV to other organs in BALB/c mice and full recovery was achieved by day 14 post-infection. Here we infected BALB/c mice IN with 10^6 PFU of MPXV-z06 and imaged them from day 2 to 14. As with CAST/EiJ mice, extensive replication was observed in the

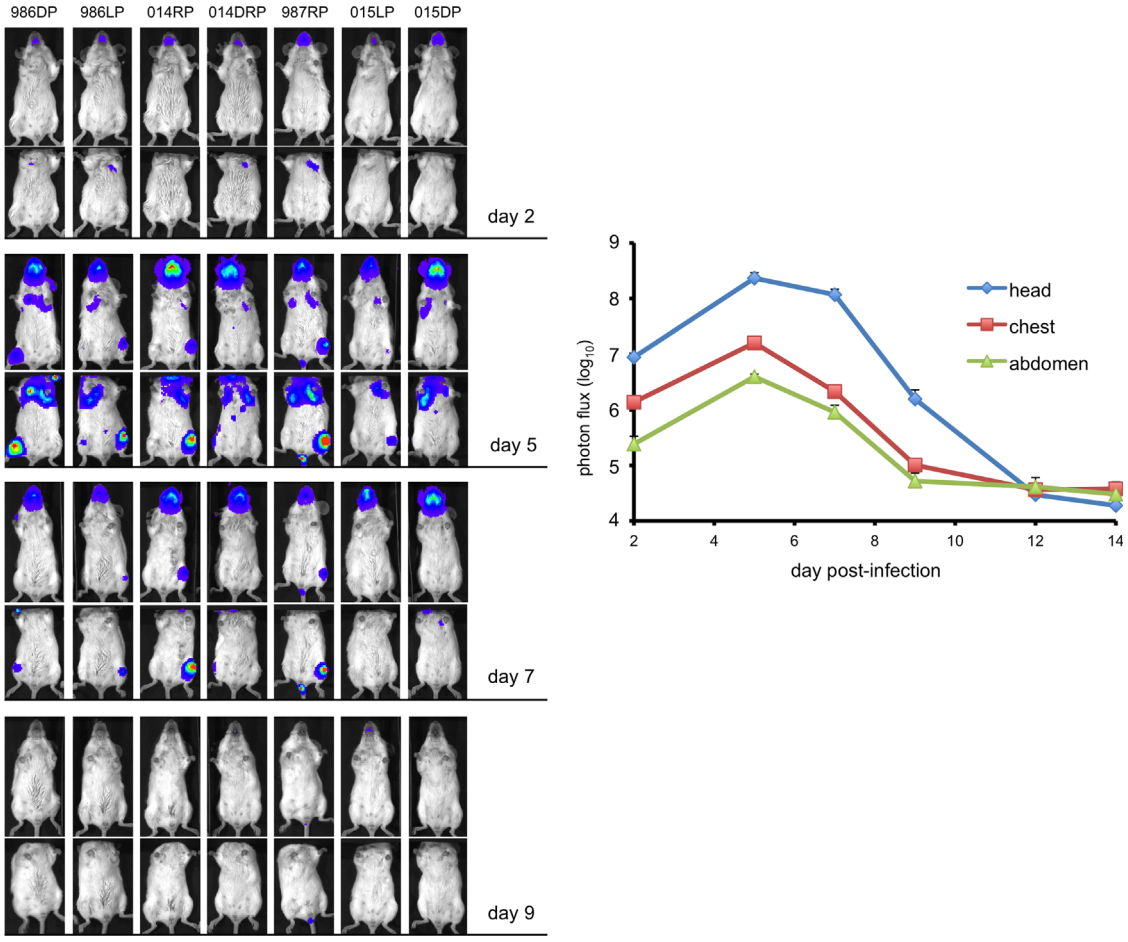

Fig. 4. Bioluminescence imaging of BALB/c mice infected with 10^6 PFU of MPXV-z06. Seven 8-week old female BALB/c mice were infected IN with MPXV-z06 and imaged every other weekday for 14 days. Exposures of whole body were 5 s at bin=8, of the covered body were 30 s at bin=8. Regions of interest defining the head, chest, and abdomen (as shown in Fig. 2) were used to determine the total photon flux. The average total photon flux for each day is shown. The experiment was performed twice with similar results.

nasal area, so images were made without and with the heads covered to allow better visualization of luminescence in the body (Fig. 4). ROIs were drawn around the head, chest, and abdomen and photon flux was calculated. For the first 5 days the photon flux in the chest and abdomen of BALB/c mice was similar to that observed for CAST/EiJ mice; however, the photon flux then rapidly decreased.

Virulence of MPXV-z06 for African dormice

Because severe infection occurred at a lower dose of MPXV in dormice compared to CAST/EiJ mice, dormice were infected with only 50, 400 and 500 PFU of MPXV-z06 by the IN route. Animals showed symptoms of lethargy, squinty eyes, ruffled coat, stiffness, and lowered body temperature. At the two higher doses, all animals succumbed between day 7 and 16 post-infection, which was later than with CAST/EiJ mice. At the lower dose of 50 PFU there was 60% survival (Fig. 5). We previously reported an LD_{50} of 12 PFU for the parental virus (Americo et al., 2010). Weight loss of up to 25% was seen in animals that received the 400 PFU dose (not shown).

Kinetics of MPXV-z06 spread in African dormice

We chose a dose of 400 PFU to infect dormice with MPXV-z06, which would be comparable to the several hundred-fold higher dose (10^4 and 10^5 PFU) used for CAST/EiJ mice with regard to lethality. Because of constraints of our breeding colony, dormice were older and varied more in age than the CAST/EiJ mice. Male dormice aged 10–12 months were infected IN and imaging was performed every 2 to 3 days. Representative luminescence images of the infected animals are shown in Fig. 6. Luminescence was first detected in the head of 4 of the 6 animals (941, 942, 946, 947) and then spread to the chest and abdomen. In 1 animal (943) luminescence was seen first in the abdomen and subsequently in the head, and in one animal (944) was seen in the head only slightly before the abdomen. The experiment in dormice was repeated with 3 females and 1 male, aged 9 to 14 months. In 3 of those animals, luminescence was first seen in the head while in the fourth animal, the chest was the primary site of replication (not shown). The more variable dissemination of MPXV in dormice contrasted with that in CAST/EiJ and BALB/c mice in which luminescence was uniformly seen first in the head. The photon flux increased more slowly during lethal infection of dormice (Fig. 6) compared to CAST/EiJ mice (Fig. 4). In addition, the photon flux was similar in head, chest and abdomen of infected dormice (Fig. 6) whereas in CAST/EiJ (Fig. 4) and BALB/c (Fig. 5) mice the amount of luminescence in the head far exceeded that in the body.

On the day of death, major organs from dormice infected with 400 PFU of MPXV-z06 were removed, and virus titers determined. High titers of MPXV were found in all major organs including lung, liver, and spleen (Figs. 6 and 7). The titers in the liver were higher than in any other organ, in most cases by more than one log. This contrasted with CAST/EiJ mice in which titers in the lungs were several logs higher than in any other organ (Fig. 7).

Discussion

BLI was useful for comparing the dissemination of MPXV in the CAST/EiJ mouse and dormouse models as it allowed us to follow the course of infection with both non-lethal and lethal doses and in which there were variations between animals. However, as previously reported (Luker et al., 2005), the ratio of photon flux to virus titer varied for different organs due in large part to the overlying tissues. In particular, light emission from the lungs was dramatically reduced such that similar photon fluxes from the chest and abdomen concealed nearly a three-log higher virus titer in the lungs compared to the liver and spleen. Therefore, the most accurate photon flux comparisons are between similar anatomic sites.

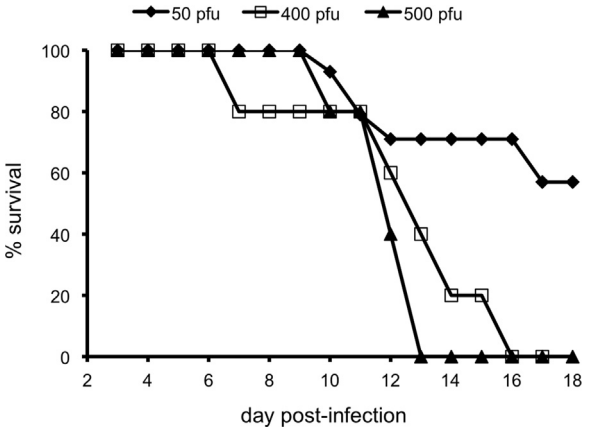

Fig. 5. Survival of African dormice infected with 50, 400, or 500 PFU of MPXV-z06. Groups of 6–10 male and female dormice aged 4 to 14 months were infected IN with MPXV-z06 and followed until death or for 32 days. Two mice, in the 400 PFU group, became moribund and were euthanized.

IN infection of CAST/EiJ mice resulted in initial MPXV replication in the nasal areas followed by spread to the lungs and other internal organs. Enhanced luminescence in the chest was detected on day 3, peaked on day 6 and declined sharply between days 14 and 18 in non-lethal infections. In lethal infections, there was no reduction in luminescence and death occurred within 10 days. Similar photon fluxes were observed in the chest and abdomen but the virus titers in the lungs were much higher than in the liver and spleen. We also imaged MPXV spread in BALB/c mice, which are much more resistant to MPXV than CAST/EiJ mice (Americo et al., 2010). Initially, the course of MPXV dissemination in BALB/c mice was similar to that of CAST/EiJ, but clearance of the infection occurred rapidly, in agreement with our previous serial sacrifice studies (Earl et al., 2012). We recently found that interferon-gamma levels in the lungs of BALB/c peaked just before MPXV clearance whereas only low levels of this cytokine were detected in the lungs of CAST/EiJ mice (Earl et al., 2012). It remains to

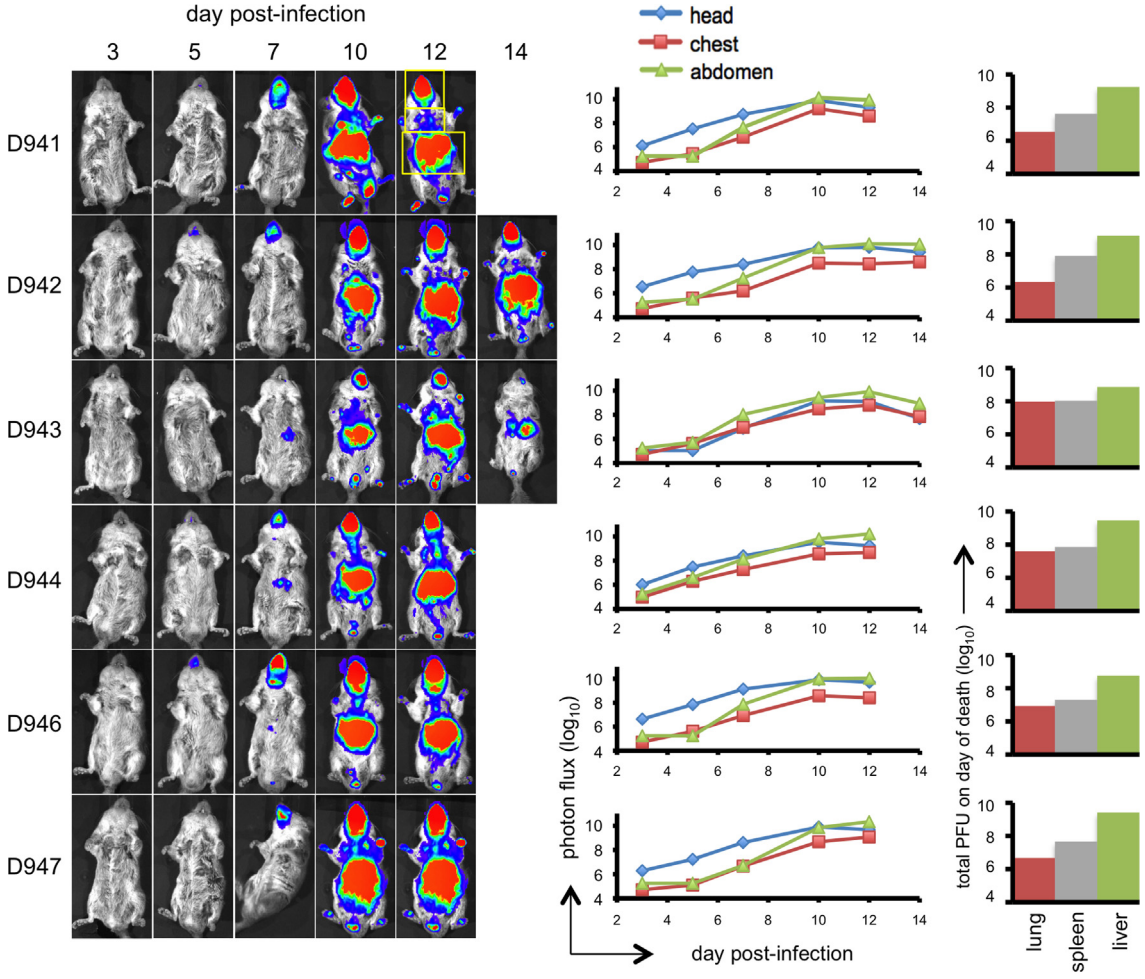

Fig. 6. Bioluminescence imaging of African dormice infected with 400 PFU of MPXV-z06. Six male dormice from 10 to 12 months of age were infected IN with MPXV-z06. Animals were imaged every other weekday from day 3 post-infection until death. Exposures were 5 s at bin=8 and all were adjusted to the same color scale. Regions of interest (yellow boxes as shown in animal D941) were drawn for quantitation of luminescence in the head, chest, and abdomen. Total photon flux in each of these areas is shown to the right of each animal. On the day of death, organs were removed and virus titers determined by plaque assay.

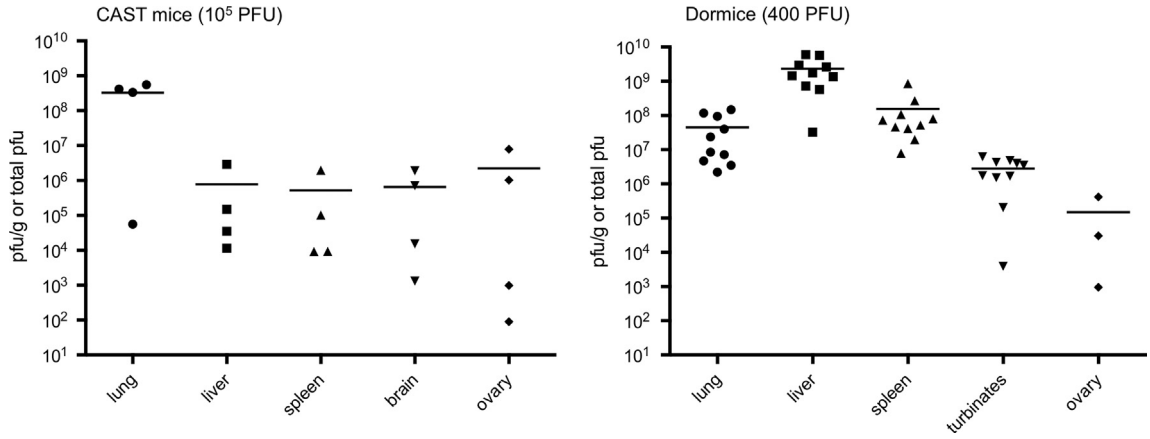

Fig. 7. Virus yield from organs of CAST/EiJ mice and African dormice infected with a lethal dose of MPXV-z06. Ten dormice (7 male and 3 female) between 9 and 14 months of age were infected IN with 400 PFU of MPXV-z06. Four 9-week old female CAST mice were infected IN with 2×10^5 PFU of MPXV-z06. On the day of death, organs were removed and virus titers were determined by plaque assay. Lung, liver, spleen, and brain are PFU/g; nasal turbinates and ovaries are total PFU.

be determined whether available reagents for detection of interferon-gamma are compatible with dormice.

Spread of MPXV occurred more slowly in dormice than in CAST/EiJ mice and the dormice exhibited greater individual variation, perhaps reflecting their outbreeding. A total of 10 African dormice ranging from 9 to 14 months were imaged, including 7 males and 3 females. No difference in clinical disease could be attributed to either age or gender. In most animals luminescence was detected in the abdomen at about the same time as in the chest and was more intense there. Furthermore, on the day of death, there were higher loads of infectious virus in the liver than other organs, a strikingly different result than with CAST/EiJ mice. It is relevant to compare the present BLI study with the analysis reported by Schultz et al. (2009) in which over 100 dormice were serially sacrificed. In the latter study, an IN dose of 2×10^4 PFU, which is approximately 1000 LD_{50} and 50X the highest dose used in our BLI. In the majority of animals MPXV was detected in nasal lavage on day 2 and lungs, liver and spleen on day 5. The highest levels of MPXV were recovered from liver on day 8, the last day that still surviving animals could be analyzed. Although the progression of the disease was accelerated at the high dose in the previous report, the dissemination to the various organs was similar to that of our study. Taken together, the data suggest that MPXV dissemination in dormice occurs through the blood or lymphatic system rather than directly from the nasal cavity to the lungs. In contrast, MPXV dissemination appears to occur from the nasal cavity directly to the lungs in both BALB/c and CAST/EiJ mice. In monkeys infected either through the aerosol, intravenous or intrabronchial route, pneumonia is prominent and more virus and pathological changes were found in lung than liver or spleen (Goff et al., 2011; Johnson et al., 2011; Zaucha et al., 2001). In humans, bronchopneumonia was diagnosed in 34 of 270 previously unvaccinated patients and tended to occur late in disease (Jezek and Fenner, 1988). However, the pathologies leading to death have not been ascertained.

The use of both CAST/EiJ mice and African dormice seems advantageous for many types of studies due to differences in the mode of MPXV spread. Clearly, CAST/EiJ mice are superior for in depth immunological studies because of the availability of reagents. However, African dormice may be a natural host with a slower course of disease.

Materials and methods

Cells

BS-C-1 cells were maintained at 37 °C and 5% CO_2 in modified Eagle minimal essential medium (EMEM; Quality Biologicals, Inc., Gaithersburg, MD) supplemented with 8% heat-inactivated fetal bovine serum (FBS), 2 mM L-glutamine, 10 U of penicillin/ml, and 10 μg of streptomycin/ml.

Recombinant virus expressing FL

All procedures with MPXV were carried out in a select agent-registered BSL-3 laboratory. The previously described clonal isolate, MPXV-z79-CB2 (Americo et al., 2010), derived from a low passage stock of MPXV-z79-I-005 originally obtained from I. Damon, CDC, Atlanta, GA, was used to construct a recombinant virus expressing the FL gene under control of an early/late synthetic promoter (Chakrabarti et al., 1997). The FL gene was inserted between the 044 and 045 open reading frames of MPXV-z79-CB2 as follows. DNA fragments with approximately 600 bp of each of the insertion flanks were created by PCR. A DNA fragment containing the FL gene controlled by a synthetic VACV early-late promoter was amplified from IHDJ-vFire (Bengali et al., 2012). The three fragments were then fused by overlap extension PCR. BSC-1 cells were infected with MPXV-z79-CB2 at a multiplicity of infection of 0.05 PFU/cell and subsequently transfected with the DNA fragment using Lipofectamine 2000 (Life Technologies, Carlsbad, CA). After 3 days, the cells were harvested by scraping, centrifuged, and resuspended in 0.5 ml of EMEM containing 2.5% FBS. A limiting dilution protocol was used to isolate virus that expressed FL. The virus was then subjected to an additional three rounds of plaque purification.

MPXV was purified by extraction with Genetron (1,1,2-trichloro-1,2,2-trifluoroethane; Chemsavers, Powhatan, VA) and centrifugation through a sucrose cushion as previously described (Americo et al., 2010).

One-step growth curve

BS-C-1 cells were infected with 3 PFU per cell of MPXV in 12-well plates. One hour after infection, monolayers were washed twice and overlaid with fresh medium. At 0, 2, 5, 8, 12, 24, 48, and 72 h after infection, cells from triplicate wells were harvested, centrifuged, suspended in fresh medium, and stored at −80 °C. Cells were lysed by three freeze-thaw cycles, sonicated and virus titered in duplicate by plaque assay on BS-C-1 cells.

Animals

CAST/EiJ and BALB/c mice were obtained from Jackson Laboratories (Bar Harbor, ME) and Taconic Biotechnology (Germantown, NY), respectively. African dormice (*Graphiurus kelleni*), originally provided by R. Buller (St. Louis University, St. Louis, MO), were

bred and maintained by the Comparative Medicine Branch, NIAID as described (Kastenmayer et al., 2010). All animals were maintained in ventilated microisolator cages.

Inoculation of animals

MPXV-z06 was diluted in phosphate-buffered saline containing 0.05% bovine serum albumin just prior to inoculation. The virus concentration of each dilution used for inoculation was verified by plaque assay. Animals were anesthetized by inhalation of isoflurane and IN infections were performed by instillation of 10–20 μl of virus into one nostril. Infected CAST/EiJ mice and dormice were housed 2 to 3 per cage and one per cage, respectively. Animals were observed daily for signs of disease and weighed daily or every other day. Most animals that succumbed to disease were found dead; none reached the euthanasia criteria of 30% weight loss. However, two African dormice were observed to be moribund and were euthanized in accordance with NIAID Animal Care and Use protocols. All animal experiments were performed in an ABSL-3 suite with approval of the NIAID Animal Care and Use Committee and the Centers for Disease Control.

Bioluminescence imaging

An IVIS 200 series system with a cooled charge-coupled-device camera (Perkin Elmer, Waltham, MA) was utilized to image animals. D-luciferin (Perkin Elmer, Waltham, MA) was injected intraperitoneally (150 μg/g body weight) 10 min prior to imaging. Animals were anesthetized with isoflurane for the duration of the imaging procedures. Images were collected every weekday or every other weekday from day 3 post-infection until death or until virus was cleared. Acquisition times were from 1 s to 1 min with varying binning factors depending on the light emission. ROI were drawn around specific anatomic sites and light emission was measured as photons/s/cm^2/sr (photon flux) using Living Image Software. Naïve animals were similarly imaged and used for background subtraction.

Titration of virus from organs

Lungs, livers, spleens, nasal turbinates, ovaries and brains were removed aseptically and placed in 2–3 ml of balanced salt solution supplemented with 0.1% bovine serum albumin and stored at −80 °C until used. Homogenization and virus plaque assays were performed as previously described (Americo et al., 2010).

Acknowledgments

We thank Gary Luker for advice regarding BLI and the NIAID Comparative Medicine Branch for care of animals. The research was supported by the Division of Intramural Research, NIAID, NIH.

References

Americo, J.L., Moss, B., Earl, P.L., 2010. Identification of wild-derived inbred mouse strains highly susceptible to monkeypox virus infection for use as small animal models. J. Virol. 84, 8172–8180.
Americo, J.L., Sood, C.L., Cotter, C.A., Vogel, J.L., Kristie, T.M., Moss, B., Earl, P.L., 2014. Susceptibility of the wild-derived inbred CAST/Ei mouse to infection by orthopoxviruses analyzed by live bioluminescence imaging. Virology 449, 120–132.
Bengali, Z., Satheshkumar, P.S., Moss, B., 2012. Orthopoxvirus species and strain differences in cell entry. Virology 433, 506–512.
Bera, B.C., Shanmugasundaram, K., Barua, S., Venkatesan, G., Virmani, N., Riyesh, T., Gulati, B.R., Bhanuprakash, V., Vaid, R.K., Kakker, N.K., Malik, P., Bansal, M., Gadvi, S., Singh, R.V., Yadav, V., Sardarilal, Nagarajan, G., Balamurugan, V., Hosamani, M., Pathak, K.M.L., Singh, R.K., 2011. Zoonotic cases of camelpox infection in India. Vet. Microbiol. 152, 29–38.
Cann, J.A., Jahrling, P.B., Hensley, L.E., Wahl-Jensen, V., 2013. Comparative pathology of smallpox and monkeypox in man and macaques. J. Comp. Pathol 148, 6–21.
Chakrabarti, S., Sisler, J.R., Moss, B., 1997. Compact, synthetic, vaccinia virus early/late promoter for protein expression. Biotechniques 23, 1094–1097.
da Fonseca, F.G., Kroon, E.G., Nogueira, M.L., Trindade, G.D., 2011. Zoonotic vaccinia virus outbreaks in Brazil. Future Virol. 6, 697–707.
Damon, I., 2007. Poxviruses. In: Knipe, D.M., Howley, P.M. (Eds.), Field's Virology, vol. 2. Lippincott Williams & Wilkins, Philadelphia, pp. 2947–2976.
Earl, P.L., Americo, J.L., Moss, B., 2012. Lethal monkeypox virus infection of CAST/EiJ mice is associated with a deficient interferon-gamma response. J. Virol. 86, 9105–9112.
Essbauer, S., Pfeffer, M., Meyer, H., 2010. Zoonotic poxviruses. Vet. Microbiol. 140, 229–236.
Esteban, D.J., Buller, R.M.L., 2005. Ectromelia virus: the causative agent of mousepox. J. Gen. Virol. 86, 2645–2659.
Falendysz, E.A., Londono-Navas, A.M., Meteyer, C.U., Pussini, N., Lopera, J.G., Osorio, J.E., Rocke, T.E., 2014. Evaluation of monkeypox virus infection of black-tailed prarie (*Cynomys Ludovicianus*) using Iin vivo bioiluminescdent imaging. J. Wildlife Dis. 50, 524–536.
Fenner, F., Henderson, D.A., Arita, I., Jezek, Z., Ladnyi, I.D., 1988. Smallpox and Its Eradication, first ed. World Health Organization, Geneva.
Goff, A.J., Chapman, J., Foster, C., Wlazlowski, C., Shamblin, J., Lin, K., Kreiselmeier, N., Mucker, E., Paragas, J., Lawler, J., Hensley, L., 2011. A novel respiratory model of infection with monkeypox virus in cynomolgus macaques. J. Virol. 85, 4898–4909.
Guarner, J., Johnson, B.J., Paddock, C.D., Shieh, W.J., Goldsmith, C.S., Reynolds, M.G., Damon, I.K., Regnery, R.L., Zaki, S.R., 2004. Monkeypox transmission and pathogenesis in prairie dogs. Emerging Infect. Dis 10, 426–431.
Hutson, C.L., Abel, J.A., Carroll, D.S., Olson, V.A., Braden, Z.H., Hughes, C.M., Dillon, M., Hopkins, C., Karem, K.L., Damon, I.K., Osorio, J.E., 2010. Comparison of West African and Congo Basin Monkeypox Viruses in BALB/c and C57BL/6 Mice. PLoS One, 5.
Hutson, C.L., Damon, I.K., 2010. Monkeypox virus infections in small animal models for evaluation of anti-poxvirus agents. Viruses 2, 2763–2776.
Hutson, C.L., Lee, K.N., Abel, J., Carroll, D.S., Montgomery, J.M., Olson, V.A., Li, Y., Davidson, W., Hughes, C., Dillon, M., Spurlock, P., Kazmierczak, J.J., Austin, C., Miser, L., Sorhage, F.E., Howell, J., Davis, J.P., Reynolds, M.G., Braden, Z., Karem, K.L., Damon, I.K., Regnery, R.L., 2007. Monkeypox zoonotic associations: insights from laboratory evaluation of animals associated with the multi-state US outbreak. Am. J. Trop. Med. Hyg. 76, 757–768.
Hutson, C.L., Olson, V.A., Carroll, D.S., Abel, J.A., Hughes, C.M., Braden, Z.H., Weiss, S., Self, J., Osorio, J.E., Hudson, P.N., Dillon, M., Karem, K.L., Damon, I.K., Regnery, R.L., 2009. A prairie dog animal model of systemic orthopoxvirus disease using West African and Congo Basin strains of monkeypox virus. J. Gen. Virol. 90, 323–333.
Jezek, Z., Fenner, F., 1988. Human monkeypox. Monogr. Virol 17, 1–140.
Johnson, R.F., Dyall, J., Ragland, D.R., Huzella, L., Byrum, R., Jett St, C., Claire, M., Smith, A.L., Paragas, J., Blaney, J.E., Jahrling, P.B., 2011. Comparative analysis of monkeypox virus infection of cynomolgus macaques by the intravenous or intrabronchial inoculation route. J. Virol. 85, 2112–2125.
Kastenmayer, R.J., Moak, H.B., Jeffress, E.J., Elkins, W.R., 2010. Management and care of African Dormice (*Graphiurus kelleni*). J. Am. Assoc. Lab. Animal Sci 49, 173–176.
Keckler, M.S., Carroll, D.S., Gallardo-Romero, N.F., Lash, R.R., Salzer, J.S., Weiss, S.L., Patel, N., Clemmons, C.J., Smith, S.K., Hutson, C.L., Karem, K.L., Damon, I.K., 2011. Establishment of the black-tailed prairie dog (*Cynomys ludovicianus*) as a novel animal model for comparing smallpox vaccines administered preexposure in both high- and low-dose monkeypox virus challenges. J. Virol. 85, 7683–7698.
Langohr, I.M., Stevenson, G.W., Thacker, H.L., Regnery, R.L., 2004. Extensive lesions of Monkeypox in a prairie dog (Cynomys sp.). Vet. Pathol. 41, 702–707.
Luker, K.E., Hutchens, M., Schultz, T., Pekosz, A., Luker, G.D., 2005. Bioluminescence imaging of vaccinia virus: Effects of interferon on viral replication and spread. Virology 341, 284–300.
Luker, K.E., Luker, G.D., 2008. Applications of bioluminescence imaging to antiviral research and therapy: multiple luciferase enzymes and quantitation. Antiviral Res. 78, 179–187.
McCollum, A.M., Damon, I.K., 2014. Human monkeypox. Clin. Inf. Dis 58, 260–267.
Moss, B., 2007. Poxviridae: the viruses and their replication (Fields Virology). In: Knipe, D.M., Howley, P.M. (Eds.), vol. 2. Lippincott Williams & Wilkins, Philadelphia, pp. 2905–2946 (2 vols).
Osorio, J.E., Iams, K.P., Meteyer, C.U., Rocke, T.E., 2009. Comparison of monkeypox viruses pathogenesis in mice by in vivo imaging. PLoS One 4, e6592.
Parker, S., Buller, R.M., 2013. A review of experimental and natural infections of animals with monkeypox virus between 1958 and 2012. Future Virol. 8, 129–157.
Parker, S., Nuara, A., Buller, R.M.L., Schultz, D.A., 2007. Human monkeypox: an emerging zoonotic disease. Future Microbiol. 2, 17–34.
Reynolds, M.G., Damon, I.K., 2012. Outbreaks of human monkeypox after cessation of smallpox vaccination. Trends Microbiol. 20, 80–87.
Reynolds, M.G., Yorita, K.L., Kuehnert, M.J., Davidson, W.B., Huhn, G.D., Holman, R.C., Damon, I.K., 2006. Clinical manifestations of human monkeypox influenced by route of infection. J. Inf. Dis 194, 773–780.
Sbrana, E., Xiao, S.Y., Newman, P.C., Tesh, R.B., 2007. Comparative pathology of North American and central African strains of monkeypox virus in a ground squirrel model of the disease. Am. J. Trop. Med. Hyg. 76, 155–164.
Schultz, D.A., Sagartz, J.E., Huso, D.L., Buller, R.M.L., 2009. Experimental infection of an African dormouse (*Graphiurus kelleni*) with monkeypox virus. Virology 383, 86–92.

Singh, R.K., Balamurugan, V., Bhanuprakash, V., Venkatesan, G., Hosamani, M., 2012. Emergence and reemergence of vaccinia-like viruses: global scenario and perspectives. Indian J. Virol. 23, 1–11.
Stittelaar, K.J., Neyts, J., Naesens, L., van Amerongen, G., van Lavieren, R.F., Holy, A., De Clercq, E., Niesters, H.G., Fries, E., Maas, C., Mulder, P.G., van der Zeijst, B.A., Osterhaus, A.D., 2006. Antiviral treatment is more effective than smallpox vaccination upon lethal monkeypox virus infection. Nature 439, 745–748.
Stittelaar, K.J., van Amerongen, G., Kondova, I., Kuiken, T., van Lavieren, R.F., Pistoor, F.H., Niesters, H.G., van Doornum, G., van der Zeijst, B.A., Mateo, L., Chaplin, P.J., Osterhaus, A.D., 2005. Modified vaccinia virus Ankara protects macaques against respiratory challenge with monkeypox virus. J. Virol. 79, 7845–7851.
Tesh, R.B., Watts, D.M., Sbrana, E., Siirin, M., Popov, V.L., Xiao, S.Y., 2004. Experimental infection of ground squirrels (Spermophilius tridecemlineatus) with Monkeypox virus. Emerging Infect. Dis 10, 1563–1567.
Xiao, S.Y., Sbrana, E., Watts, D.M., Siirin, M., da, R.A., Tesh, R.B., 2005. Experimental infection of prairie dogs with monkeypox virus. Emerging Inf. Dis 11, 539–545.
Zaitseva, M., Kapnick, S.M., Scott, J., King, L.R., Manischewitz, J., Sirota, L., Kodihalli, S., Golding, H., 2009. Application of bioluminescence imaging to the prediction of lethality in vaccinia virus-infected mice. J. Virol. 83, 10437–10447.
Zaucha, G.M., Jahrling, P.B., Geisbert, T.W., Swearengen, J.R., Hensley, L., 2001. The pathology of experimental aerosolized monkeypox virus infection in cynomolgus monkeys (*Macaca fascicularis*). Lab. Invest. 81, 1581–1600.